l'Observatoire de Paris — BNM-SYRTE — Systèmes de Référence Temps Espace — BNM Bureau National de Métrologie — CNRS Centre National de la Recherche Scientifique

FREQUENCY COMPARISON (H_MASER 1400805) - (BNM-SYRTE-FO2)
From MJD 53379 to MJD 53399

The primary frequency standard BNM-SYRTE-FO2 was compared to the hydrogen Maser (1400805) of the laboratory, from MJD 53379 to MJD 53399.

The mean frequency differences measured between the hydrogen Maser 1400805 and fountain FO2 during this period is given in table 1. Additionally, the mean frequency between hydrogen Masers 1400816 and 1400805 are evaluated during the same period of measurement.

Period (MJD)	y(HMaser$_{1400805}$ - FO2) (1)	u_B (2)	u_A (3)	$u_{link\ /\ maser}$ (4)
53379 – 53399	**+ 6393,11**	**7,57**	**0,42**	**1,03**
53379 - 53399	**y(HMaser$_{1400805}$- HMaser$_{1400816}$)** **+3298,24** (8)	**0,022**	**0,037**	

Table 1: Results of the comparison in 1 x 10^{-16} unit.

Figure 1 collects the measurements of fractional frequency differences during the 9th to 29th January period. The measurements are corrected for the systematic frequency shifts listed below.

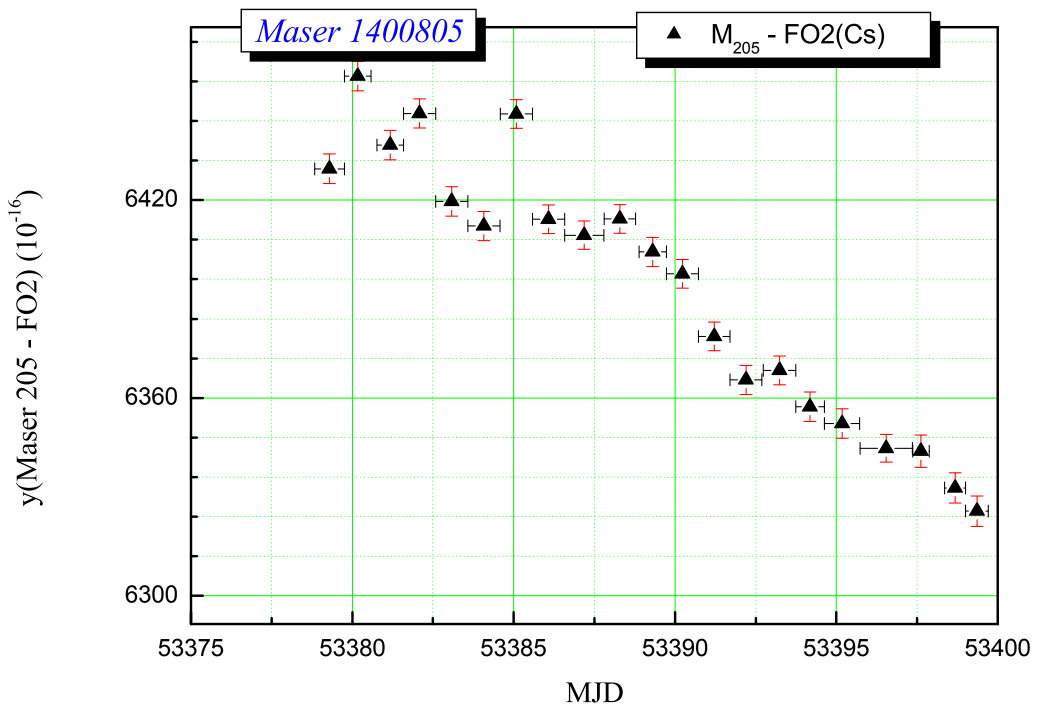

Figure 1: fractional frequency differences between H_Maser1400816 & FO2 from MJD 53379 to MJD 53399

Table of measurements is given bellow (table 2).

Start UTC dates unit MJD	Start Local dates unit H:M	Duration H :M	Mean fractional frequency differences $y_{Maser} - y_{FO2}$	type A uncertainties σ_{Stat}	$\sigma_{Collision}$
53378,82986	08/01/2005 20:55	22:11	6,42952E-13	1,31E-16	1,69E-16
53379,75417	09/01/2005 19:06	19:52	6,45756E-13	1,3E-16	1,66E-16
53380,76597	10/01/2005 19:23	19:36	6,43668E-13	1,28E-16	1,61E-16
53381,58264	11/01/2005 14:59	24:01	6,44627E-13	1,15E-16	1,54E-16
53382,58333	12/01/2005 15:00	23:57	6,41961E-13	1,29E-16	1,66E-16
53383,58125	13/01/2005 14:57	23:49	6,41212E-13	1,22E-16	1,57E-16
53384,58056	14/01/2005 14:56	24:03	6,44615E-13	1,19E-16	1,51E-16
53385,58264	15/01/2005 14:59	24:01	6,41419E-13	1,17E-16	1,48E-16
53386,58333	16/01/2005 15:00	28:55	6,40933E-13	1,07E-16	1,38E-16
53387,79792	17/01/2005 20:09	23:25	6,41431E-13	1,18E-16	1,53E-16
53388,88403	18/01/2005 22:13	20:15	6,40431E-13	1,23E-16	1,6E-16
53389,72847	19/01/2005 18:29	23:55	6,39761E-13	1,16E-16	1,46E-16
53390,725	20/01/2005 18:24	23:34	6,37865E-13	1,17E-16	1,49E-16
53391,70694	21/01/2005 17:58	23:36	6,36547E-13	1,19E-16	1,55E-16
53392,73611	22/01/2005 18:40	24:08	6,36839E-13	1,17E-16	1,48E-16
53393,74167	23/01/2005 18:48	21:14	6,35735E-13	1,32E-16	1,66E-16
53394,62778	24/01/2005 16:04	26:17	6,35221E-13	1,32E-16	1,72E-16
53395,73333	25/01/2005 18:36	39:03	6,34473E-13	8,99E-17	1,15E-16
53397,3625	27/01/2005 09:42	12:17	6,34386E-13	1,78E-16	2,32E-16
53398,35625	28/01/2005 09:33	15:37	6,33272E-13	1,46E-16	1,88E-16
53399,00694	29/01/2005 01:10	16:55	6,32567E-13	1,49E-16	1,93E-16

Table 2: Measurements H_Maser1400805 - FO2 from MJD 53379 to 53399

Start UTC dates unit MJD	Stop UTC dates unit MJD	Duration & Measurement Rate	Mean frequency difference normalized $y_{Maser} - y_{FO2}$ **(1)**	type A uncertainty σ_{Stat} & $\sigma_{Collision}$	Uncertainty due to the dead times $\sigma_{deadTime}$ **(4)**
53378,82986	53399,71181	Total duration : 20,88195 d Total measurements 20.018 d Measurement Rate: 95,86 %	Standard Mean $\bar{y}$ = **6393,17** x **10^{-16}** Weighted Mean **(5)**: $\bar{y}$ = **6394,61 x 10^{-16}** Linear fit regression **(6)**: $\bar{y}$ = **6393,12 x 10^{-16}** High order polynomial fit **(6)**: $\bar{y}$ = **6389,29x 10^{-16}** Mean from Phase differences **(7)**: $\bar{y}$ = **6393,11 x 10^{-16}**	σ_A = 0,**434** x **10^{-16} (3)** Linear fit regression**(6)** σ_y = 2,**47** x **10^{-16}** High order Polynomial fit **(6)** σ_y = 2,**17** x **10^{-16}** From Phase differences σ_A = 0,**42** x **10^{-16}**	$\sigma_{deadTime}$ = **1,03 10^{-16}**

Table 3: Statistics of measurements

(1) Fractional frequency difference obtained after systematic relative frequency shifts correction:

$$y_{Maser-FOM} = \frac{\delta(\nu)_{Zeeman2}}{\nu_0} + \frac{\delta(\nu)_{BlackBody}}{\nu_0} + \frac{\delta(\nu)_{Collision + CavityPulling}}{\nu_0} + \frac{\delta(\nu)_{redshift}}{\nu_0} - \frac{f_{mesure}}{\nu_0}$$

with $\nu_0 := 0.9192631770\ 10^{10}$. The fractional mean frequency is calculated by four ways as mentioned in table 3 in order to have comparison between statistical computation such as standard mean, weighted mean, with a linear fit and with phase differences.

(2) Systematic uncertainty $\sigma_B = u_B$ in witch statistical effect of cold collisions and cavity pulling is removed (see **Annexe 1**)

$$\sigma_B = \left(\sigma_{Zeeman2}^2 + \sigma_{BlackBody}^2 + \sigma_{Collision_{Syst}}^2 + \sigma_{Microwave\_Spectrum}^2 + \sigma_{Microwave\_Leakage}^2 + \sigma_{Ramsey\_Rabi}^2 + \sigma_{Recoil}^2 + \sigma_{second\_Doppler}^2 + \sigma_{Background\_collsions}^2 + \sigma_{Redshift}^2\right)^{(1/2)}$$

(3) Statistical uncertainty $\sigma_A = u_A$, in which is taken into account the statistical uncertainty on each measurement σ_{Stat_i} and statistical effect on the cold collisions and Cavity Pulling measurement $\sigma_{Collision_i}$ (see **Annexe 4** Linear Regression on the frequency measurements & **Annexe 5**) : $\sigma_A = \sqrt{\dfrac{1}{\displaystyle\sum_{i=1}^{n} \frac{1}{\sigma_{Stat_i}^2 + \sigma_{Collision_i}^2}}}$

(4) Uncertainty due to the link between H_Maser and the fountain FO2 $u_{link\_Maser} = \sqrt{\sigma_{link\_Lab}^2 + \sigma_{dead\_time}^2}$ where $\sigma_{link\_Lab} = 0.1\ 10^{-15}$ and σ_{dead_time} is the uncertainty due to the dead times during measurements (see **Annexe 3**)

(5) Weighted Mean by statistical uncertainty on each measurement

$$y_j := \frac{\displaystyle\sum_{i=1}^{n_j} \frac{y_i}{\sigma_{Ai}^2}}{\displaystyle\sum_{i=1}^{n_j} \frac{1}{\sigma_{Ai}^2}}$$

where

$$\sigma_{A_i} = \frac{1}{\sqrt{\dfrac{1}{\sigma_{Stat_i}^2 + \sigma_{Col_i}^2}}}$$

(6) Mean frequency obtained by a linear fit by weighted least squares with statistical uncertainty on each measurement and by an high order polynomial fit (see **Annexe 4**).

(7) Mean frequency obtained by phase differences that is the retained result (see **Annexe 5**).

(8) Mean frequency obtained by phase differences between Masers 1400805 and 1400816 (see **Annexe 6**).

ANNEXE 1

Uncertainties of systematic effects in the FO2 fountain

Systematic effects taken into account are the quadratic Zeeman, the Black Body, the cold collision and cavity pulling corresponding to the systematic part (see annexe 2), the microwave spectral purity and the microwave leakage, the Ramsey Rabi pulling, the recoil, the 2^{nd} Doppler and the background collisions. Each of these effects is affected by an uncertainty. The uncertainty of the red shift effect is also included in the systematic uncertainty budget and gives

$$\sigma_B = \left(\sigma_{Zeeman2}{}^2 + \sigma_{BlackBody}{}^2 + \sigma_{Collision_{Syst}}{}^2 + \sigma_{Microwave\_Spectrum\_Leakage}{}^2 + \sigma_{first\_Doppler}{}^2 + \sigma_{Ramsey\_Rabi}{}^2 + \sigma_{Recoil}{}^2 + \sigma_{second\_Doppler}{}^2 + \sigma_{Background\_collisions}{}^2 + \sigma_{Redshift}{}^2 \right)^{(1/2)}$$

Here are mentioned the uncertainties of the different effects (see **Annexe 2** and **[ref, 1]**):

Quadratic Zeeman effect	:	$\sigma_{Zeeman2} := 0.143\ 10^{-16}$	(continuously measured)
Black Body effect	:	$\sigma_{BlackBody} := 0.25\ 10^{-15}$	(calculated)
Systematic Collisional effect	:	$\sigma_{Collision_{Syst}} = 0.34778\ 10^{-15}$	(continuously measured)
Microwave Spectrum purity & Leakage effect	:	$\sigma_{Microwave\_Spectrum\_Leakage} := 0.45\ 10^{-15}$	(measured)
First order Doppler effect	:	$\sigma_{first\_Doppler} := 0.38\ 10^{-15}$	(calculated and measured)
Rabi-Ramsey effect	:	$\sigma_{Ramsey\_Rabi} < 0.10\ 10^{-15}$	(calculated)
Recoil effect (see **[ref, 3]**)	:	$\sigma_{Recoil} := 0.10\ 10^{-15}$	(calculated)
Second order Doppler effect	:	$\sigma_{second\_Doppler} := 0.8\ 10^{-17}$	(calculated)
Background effect	:	$\sigma_{Background\_collisions} := 0.10\ 10^{-15}$	(evaluated)
Red shift effect	:	$\sigma_{Redshift} = 0.1\ 10^{-15}$	(calculated)

For the whole July period it gives

➔ $\boxed{\sigma_B = 0.757\ 10^{-15}}$

ANNEXE 2

1 - Measurement of the collisional frequency shift and the cavity pulling

Collisional shift takes into account the effect of the collisions between cold Caesium atoms and the effect of "Cavity Pulling" whose influence also depends on the number of atoms. This effect is measured in a differential way during each integration and its determination thus depends on the duration of the measurement and on the stability of the clock, thus the uncertainty on the determination of the collisional shift is mainly of statistical nature. To the statistical uncertainty, we add a type B uncertainty of 1% of frequency shift resulting from the imperfection of the adiabatic passage method (see the article **[ref. 4]**).

Figure 2 visualizes the relative frequency shift due to the effect of the collisions and "Cavity Pulling" of the atomic fountain FO2 taken in low density, between the MJD 53379 and 53399 with the statistical uncertainty of each measurement, $\sigma_{Collision(i)}$ given in table 2.
Figure 3 shows the Allan deviation of a differential measurement using high and half atom density fountain configurations during MJD 53202 (from MJD 53202,72361 to MJD 53206,00278), in order to correct of the cold collisional shift for this period. FO2 was operated alternatively (every 50 clock cycles) at low atomic density (red circle) and high density (black square) against the cryogenic oscillator weakly phase locked on the H_Maser. The measured density ratio between low and high densities is **0,50001666±0,000033**. The frequency difference between both densities is used to determine the collisional coefficient which is used to correct each data point. The blue triangle points represent the Allan deviation of the frequency difference between low and high densities when the points are corrected. The Allan deviation varies as $\tau^{-1/2}$and reaches 10^{-16} after 100000s.

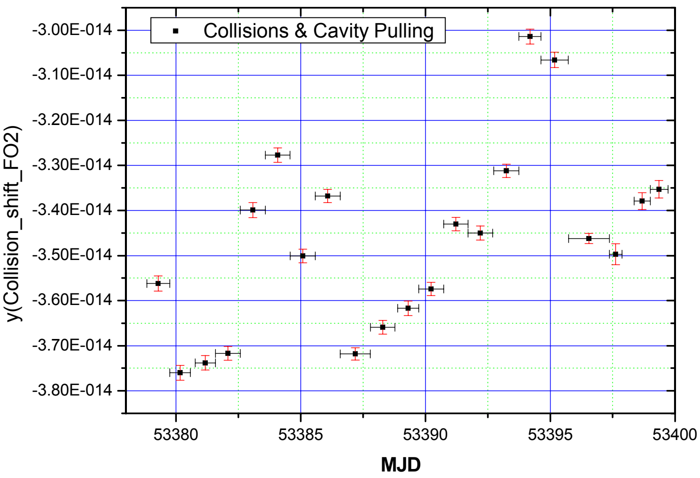

Figure 2: Fractional frequency shift due to cold collisions and Cavity Pulling from MJD 53379 to MJD 53399

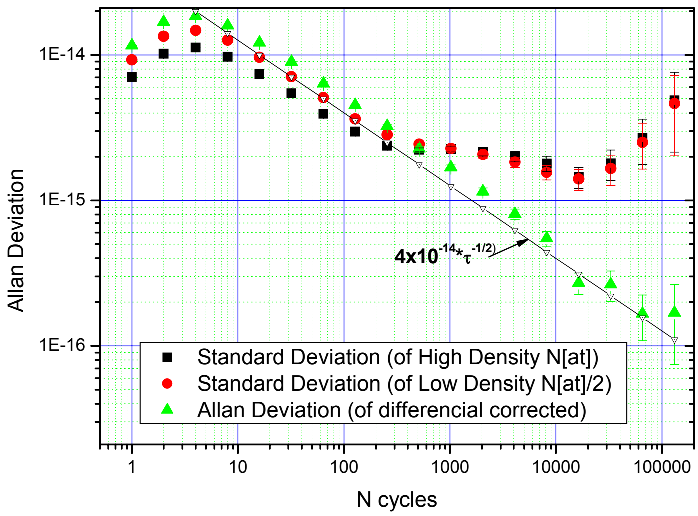

Figure 3: Allan deviation of measurements of the shift frequency in high and low atom density and their differences during MJD 53309,5 to MJD 53324,83333

The weighted mean $y_{Collision_{moy}} = \dfrac{\sum_{i=1}^{n} \dfrac{y_{Collision_i}}{\sigma_{Collision_i}^2}}{\sum_{i=1}^{n} \dfrac{1}{\sigma_{Collision_i}^2}}$ of collisionnal shift gives for January is $y_{Collision_{moy}} = -0.347780\ 10^{-13}$

The systematic effect of these shifts is evaluated by the 1% part of the mean frequency collisional shift during January:

$$\sigma_{Collision_{Syst}} = \frac{1}{100}\left|y_{Collision_{moy}}\right| = \sigma_{Collision_{Syst}} = 0.34778\ 10^{-15}$$

This value is taking into account in the systematic uncertainty evaluation σ_B (see annexe 1).

2 - Measurement of the 2nd order Zeeman frequency shift

Every 15 minutes the frequency of the central fringe of the field linearly dependant transition |F=3, m_F=1⟩ ⟶ |F=4, m_F=1⟩ is measured. This frequency is directly proportional to the field as $\delta(\nu_{11})=K_{Z1}B$ with K_{Z1} = 7,0084 Hz.nT^{-1} (see **[ref. 5]** vol. 1 p37 table 1.1.7(a)). In the fountain, the transition |F=3, m_F=0⟩ ⟶ |F=4, m_F=0⟩ is shifted by quadratic Zeeman effect and depend on squared magnetic field as $\delta(\nu_{00})=K_{Z2}B^2$ with K_{Z2} = 42,745 mHz.µT^{-2} (see **[ref. 5]** vol. 1 p37 table 1.1.7(a)). Knowing K_{Z1} and measuring δ(ν11) allow good estimation of Zeeman quadratic shift as $\delta(\nu_{00})=K_{Z2}\left(\frac{\delta(\nu_{11})}{K_{Z1}}\right)^2$. The relative quadratic Zeeman frequency shift is calculated by $\frac{\delta(\nu_{00})}{\nu_0}=427{,}45\times10^{-6}\left(\frac{\delta(\nu_{11})}{700{,}84}\right)^2$ with $\delta(\nu_{11})$ in Hz unit and ν_0 = 9192631770 Hz. And the uncertainty is evaluated by $\frac{\Delta(\delta(\nu_{00}))}{\nu_0}=427{,}45\times10^{-6}\times\frac{2\times\overline{B}\times\Delta(B)}{\nu_0}$ with B in mG. Figure 4 displays the tracking of the central fringe during MJD 53379 to MJD 53399. This shows the good stability of the magnetic field in the interrogation zone. The frequency variation is taken as in an interval of standard deviation ±0,0534Hz. When taking the standard deviation of variation of the magnetic field Δ(B) over the whole measurement period as the field uncertainty, we find 7,6 pT. The corresponding uncertainty of the correction of the second order Zeeman effect is **0,143x10^{-16}**. During each period of about 24h of integration (see table 2) an evaluation of the Zeeman effect is calculated assorted with an uncertainty averaged from the tracking of the central fringe during this interval duration of about 24h.

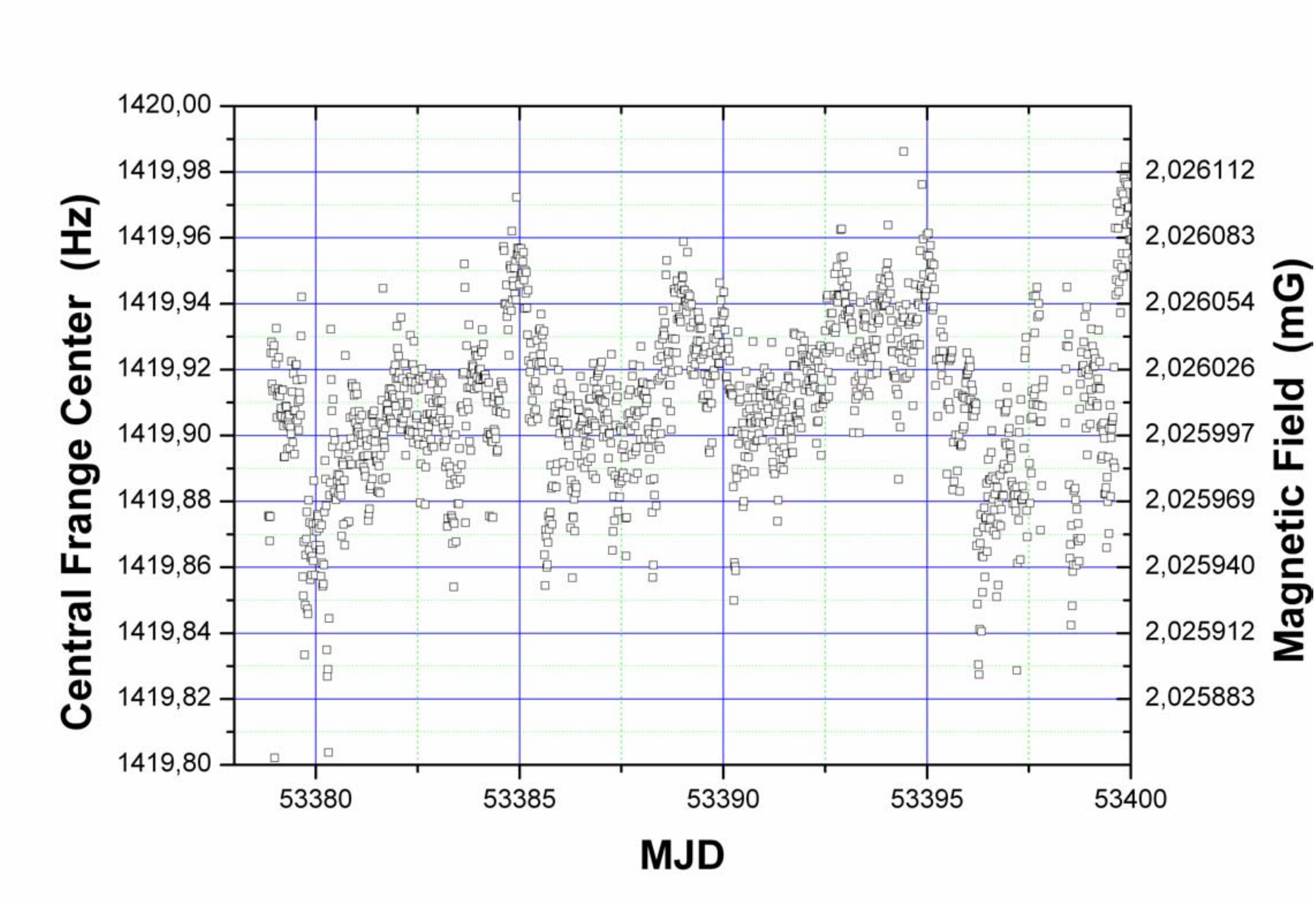

Figure 4: tracking of the central fringe from MJD 53379 to MJD 53399

3 - Measurement of the Blackbody Radiation shift

An ensemble of 3 platinum thermistors monitors the temperature and its gradient inside the vacuum chamber. The average temperature is ~25,5°C with a gradient smaller than 1 K along the atom trajectory. The correction is

$$\left(\frac{\delta(\nu)}{\nu_0}\right)_{Blackbody} = -\frac{0.0001573\left(\frac{T}{300}+0.9105000000\right)^4}{\nu_0} = -0.168281\ 10^{-13} \pm 0.25\ 10^{-15}$$

4 - Effect of the Microwave Spectrum effect and leakage effect

The clock frequency is measured as a function of the microwave power. Every 50 cycles the atom interrogation is alternated between 4 configurations of π/2, low density and high density, and 3π/2, low density and high density. It allows extrapolating and removing the variation of the collision shift in the comparison between π/2 and 3π/2 pulses. We find

$$\frac{\delta(\nu)_{Microwave\_Spectrum\_Leakage}}{\nu_0} = -0.44\ 10^{-15} \pm 0.45\ 10^{-15}$$

5 - Measurement of the residual 1st order Doppler effect

We determined the frequency shifts caused by asymmetry of the coupling coefficients of the two microwave feedthroughs and the error on the launching direction by coupling the interrogation signal either "from the right" or "from the left" or symmetrically into the cavity. The measured shift is

$$\left(\frac{\delta(\nu)}{\nu_0}\right)_{first\_Doppler} = 0.45\ 10^{-14} \pm 0.38\ 10^{-15}$$

In FO2 fountain we feed the cavity symmetrically at 1% level both in phase and in amplitude. This shift is thus reduced by a factor of 100 and became negligible. The quadratic dependence of the phase becomes dominant. A worse case estimate based on **[ref. 6]** gives fractional frequency shift of 3 x 10^{-16} which we take as uncertainty due to the residual 1st order Doppler effect.

6 – Rabi and Ramsey effect and Majorana transitions effect

An imbalance between the residual populations and coherences of $m_F < 0$ and $m_F > 0$ states can lead to a shift of the clock frequency estimated to few 10^{-18} for a population imbalance of 10^{-3} that we observe in FO2 (see **[ref. 7]** and **[ref. 8]**).

7 – Microwave recoil effect

The shift due to the microwave photon recoil was investigated in **[ref. 3]**. It is smaller than 1,4 x 10^{-16} .

8 – Gravitational red-shift and 2nd order Doppler shift

The relativistic effect is evaluated as: $\frac{\delta(\nu)_{redshift}}{\nu_0} = 0.625\ 10^{-14}$ with an uncertainty $\sigma_{Redshift} = 0.1\ 10^{-15}$

The 2nd order Doppler shift is less than 0,08 x 10^{-16} .

9 – Background collisions effect

The vacuum pressure inside the fountains is typically a few 10^{-8} Pa. Based on early measurements of pressure shift (see **[ref. 5]**) the frequency shift due to collisions with the background gas is < 10^{-16}.

See **[ref. 9]** for recent evaluations of systematic effects of FO2 fountain.

ANNEXE 3

Uncertainty due to the dead time during the measurements

A statement of the distribution of the idle periods of measurements of FO2 is represented in figure 5,

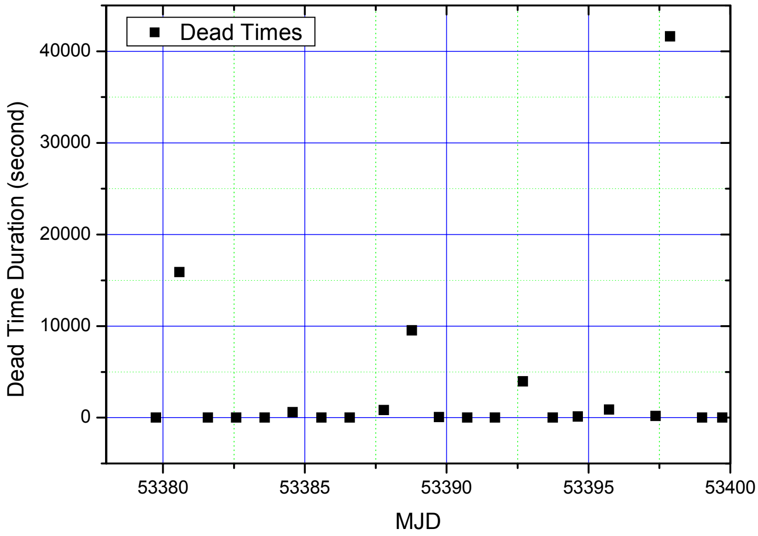

Figure 5: Dead Times on measurements of y(H_ Maser1400816 –FO2) over the period MJD 53379 to 532399

For the period of the MJD 53334 until the MJD 53401, the variations of phase between hydrogen Maser 1400805 and the hydrogen Maser 1400816 were sampled every 100s. After removing a quadratic fit on phase variations to carry out the calculation of standard deviation in the temporal field, we have evaluated the uncertainty associated with the H_Maser according to time (by step of 100s). We have obtained the phase variations between H_Maser 1400805 and the H_Maser 1400816 plotted in figure 6.

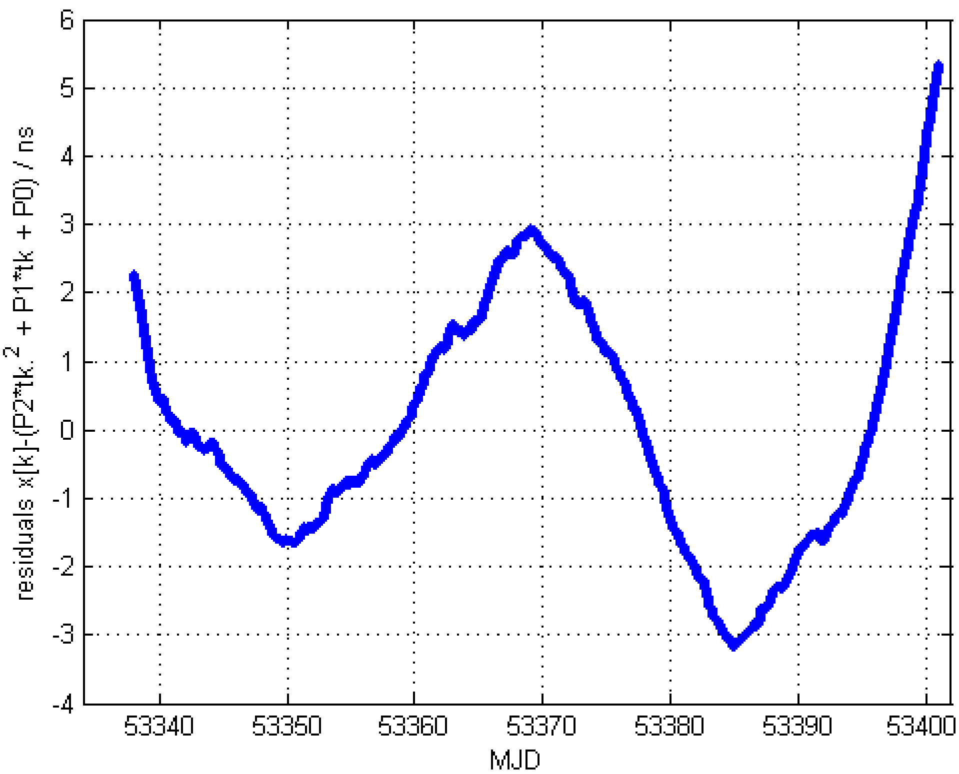

Figure 6: phase data x(Maser805-Maser816) linear drift removed x(H805-H816) MJD 53334 to MJD 53401

Frequency stability analyzes were performed using the overlapping Allan deviation on frequency data and represented for January 2005 in figure 7 and similarly time stability analyzes with a time deviation were computed and represented for january in figure 8 .

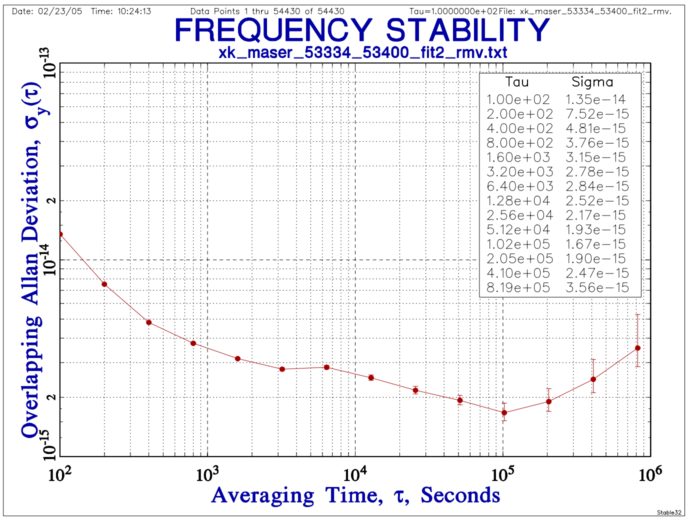

Figure 7: frequency stability analyzes x(HMaser805 - HMaser816) from MJD 53334 to MJD 53401

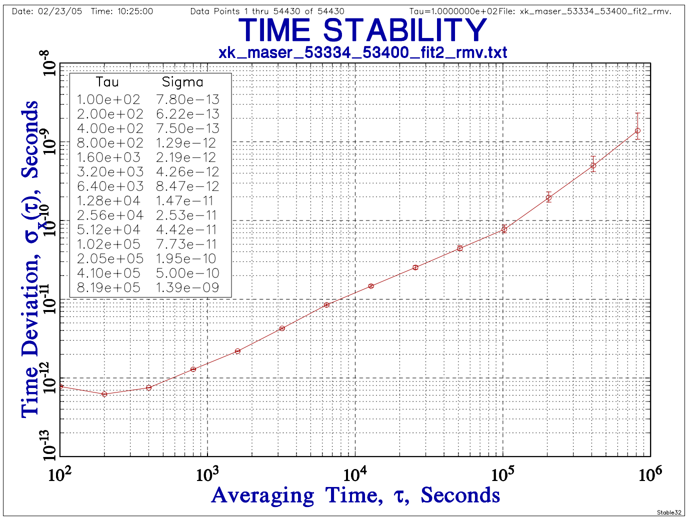

Figure 8: time stability analyzes from x(HMaser805 - HMaser816) from MJD 53334 to MJD 53401

Table 4 provides the standard deviations of the phase fluctuations of the hydrogen Maser 1400805 with respect to the hydrogen Maser 1400816 associated to each dead time according to their duration for January 2005. The quadratic sum gives

$$\sum_{i=1}^{21} \sigma_{x_i}(\tau)^2 = 0.1791169735\ 10^{-20}$$

The January 2005 period of FO2 measurements is 20,88195 days or $T := 0.180420048\ 10^{7}$ seconds. We find the standard deviation of the fluctuations of frequency due to the dead times in measurements by the ratio

$$\sigma_{deadTime} = \frac{\sqrt{\sum_{i=1}^{21} \sigma_{x_i}(\tau)^2}}{T} = \sigma_{deadTime} := 0.2346\ 10^{-16}$$

With taking $\sigma_{link\_Maser} = \sqrt{\sigma_{link\_lab}^2 + \sigma_{deadTime}^2}$ one obtains $\boxed{\sigma_{link\_Maser} = 0.1027\ 10^{-15}}$

End Date of each measurement (MJD)	Dead Time Duration second	σ_x
53379,75417	0	7,7028e-013
53380,58194	15899,99998	1,722e-011
53381,58264	0	7,7028e-013
53382,58333	0	7,7028e-013
53383,58125	0	7,7028e-013
53384,57361	600	1,0047e-012
53385,58264	0	7,7028e-013
53386,58333	0	7,7028e-013
53387,78819	839,99999	1,2721e-012
53388,77361	9539,99999	1,1779e-011
53389,72778	60,00004	7,7028e-013
53390,725	0	7,7028e-013
53391,70694	0	7,7028e-013
53392,69028	3960,00001	5,4288e-012
53393,74167	0	7,7028e-013
53394,62639	119,99999	7,7028e-013
53395,72292	899,99999	1,4003e-012
53397,36042	180,00003	6,0913e-013
53397,87431	41640,00001	3,7198e-011
53399,00694	0	7,7028e-013
53399,71181	0	7,7028e-013

Table 4: Statement of the dead times of H_Maser 1400805 - FO2 measurements between MJD 53339 and MJD 53399

ANNEXE 4

Linear Regression on the frequency measurements on period MJD 53379-53399

One calculates the linear regression by the algorithm of weighted least squares by statistical uncertainty of each frequency differences measurements:

$$y_k = a_1 + a_2\, t$$

Figure 9 gives the representation of frequency measurements and the linear fit resulting from weighted least squares by inverse of squares statistical uncertainty $1/\sigma_{Ai}^{2}$.

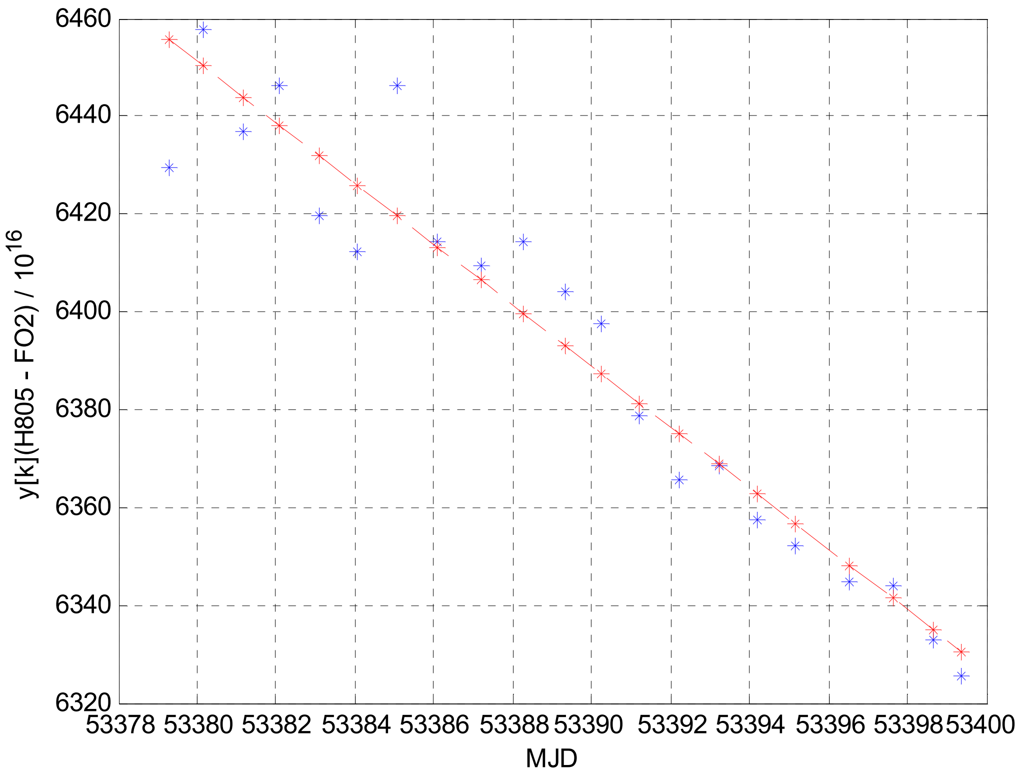

Figure 9: linear regression on the frequency y(HMaser-FO2) between MJD 53379 and 53399 weighted by uncertainty : $1/\sigma_{Ai}^{2}$

Summary of statistical terms:
Coefficient a1 = 3,39179038759808e-011 sigma(a1) des yk de FO2 = 3,96825649433859e-013
Coefficient a2 = -6,23319205204034e-016 sigma(a2) des yk de FO2 = 7,43271091693215e-018
Covariance Matrix :
1,57470596048604e-025 -2,94949031898837e-030
-2,94949031898837e-030 5,52451915746823e-035
mean date of measurements = 53389,325695
Frequency mean by linear fit y_FO2 = 6,39311817394116e-013
Uncertainty propagation at t_moyen uc_y_FO2 = 4,34823403743264e-017
Degree of Freedom DEF = 19
Mean Square Error = Chi2/DEF = 33,3669681398143
Birge ratio Rb (chi2/DEF)^1/2 = 5,7764148171521
Limit of Birge ratio Rb = 1+sqrt(2/DEF) = 1,32444284226153
Probability of a sample y(Maser-FO2) being superior of Chi2|DEF = 1,643779859728764e-122
SSR Sum Square of Residues = 2,55069604766449e-029
RMS Root Mean Square of Residues = 5,05044161204195e-015
Allan Deviation at T with assumption of White Frequency Noise = 2,47128125123936e-016
T (secondes) = total duration + tau0 = 1890114,78857167
Phase difference on the period of integration = 1,15344525256676e-006
tau0 (mean time between measurements) = 85914,3085714396 (seconds)

High order Polynomial fit on the frequency measurements on period MJD 53379-53399

One calculates the polynomial fit by the algorithm of least squares on each frequency differences measurements:

$$y = \sum_{i=0}^{M} p_{i+1} \, t^{(M-i)}$$

For data measurements we have the figure 10, 21 points with a mean time interval duration of 85914 seconds during MJD 53379-53399 periods. With a polynomial of order M=11 we have smoothed the maser noise on about 1/2 day. We obtain the polynomial fit represented on figure 11.

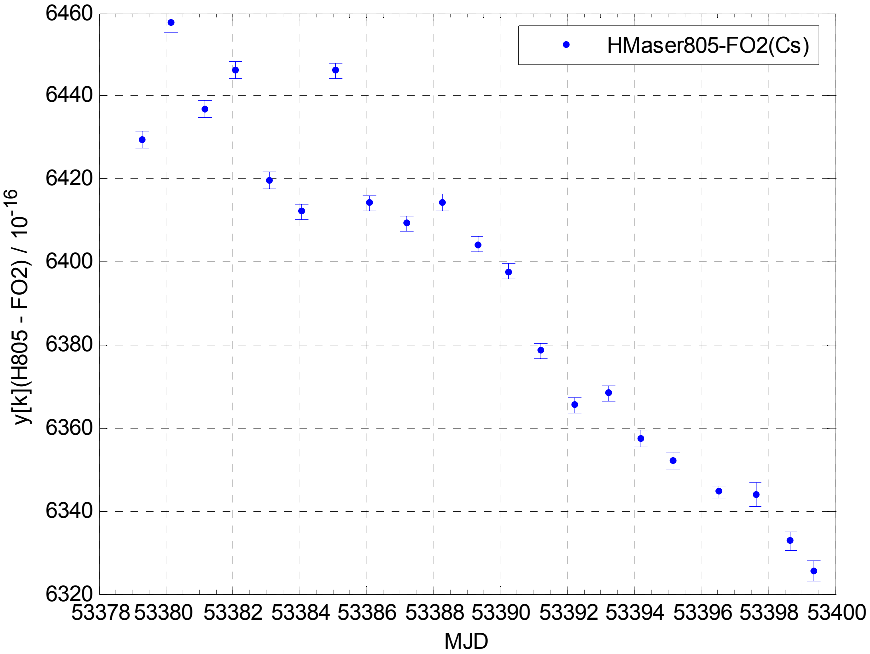

Figure 10: frequency differences averaged on about 1 day of measurements y(H805-FO2) MJD 53379 - 53399

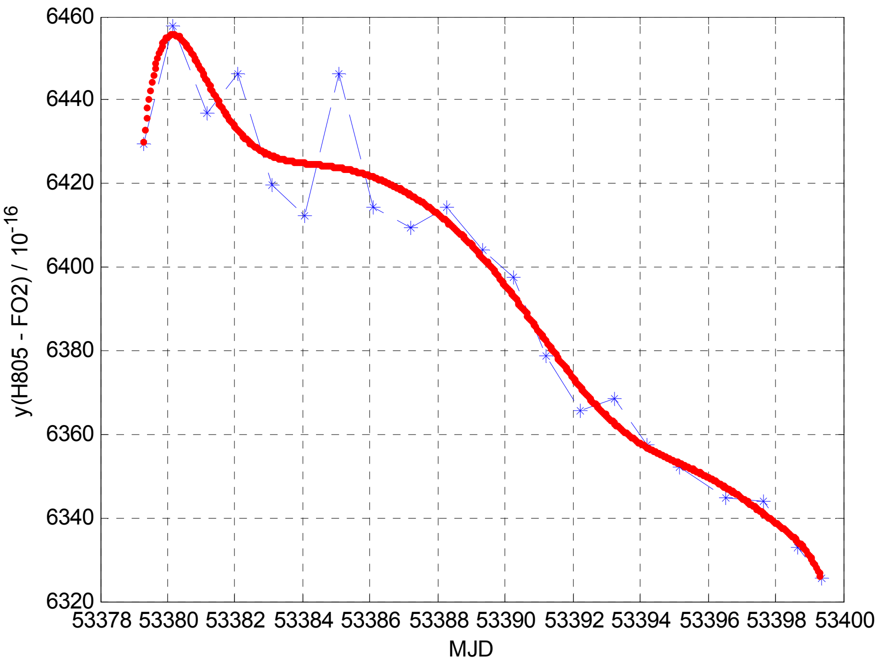

Figure 11: frequency differences y(H816-FO2) and the order 11 polynomial fit MJD 53379 - 53399

By integrating the fit polynomial from 53379 to 53399 we obtain an averaging frequency $\mathbf{y_{moy(H805\text{-}FO2)} = 6389{,}29 \times 10^{-16}}$.

Statistical uncertainty is evaluated by the frequency stability analysis of residuals. Figure 12 shows an overlapping Allan deviation and a law of white noise frequency modulation of 2,8 x $10^{-13}\tau^{-1/2}$. An extrapolated value until 20 days is obtained by this law:

$$\sigma_y(\tau=20d) = 2,13 \times 10^{-16}$$

This value is added with the statistical uncertainty σ_A obtained from each measurement

$$\sigma_A = \sqrt{\frac{1}{\sum_{i=1}^{n} \frac{1}{\sigma_{Stat_i}^2 + \sigma_{Collision_i}^2}}}$$

and resulting in σ_A = **0,434** x **10^{-16}** and finally the statistical uncertainty of mean frequency $\mathbf{y_{moy(H816-FO2)}} = \mathbf{6389,29 \times 10^{-16}}$:

$$u_A = \sqrt{\sigma_A^2 + \sigma_y(\tau = 20\,d)^2}$$

$$\boxed{u_A = 0.21739\ 10^{-15}}$$

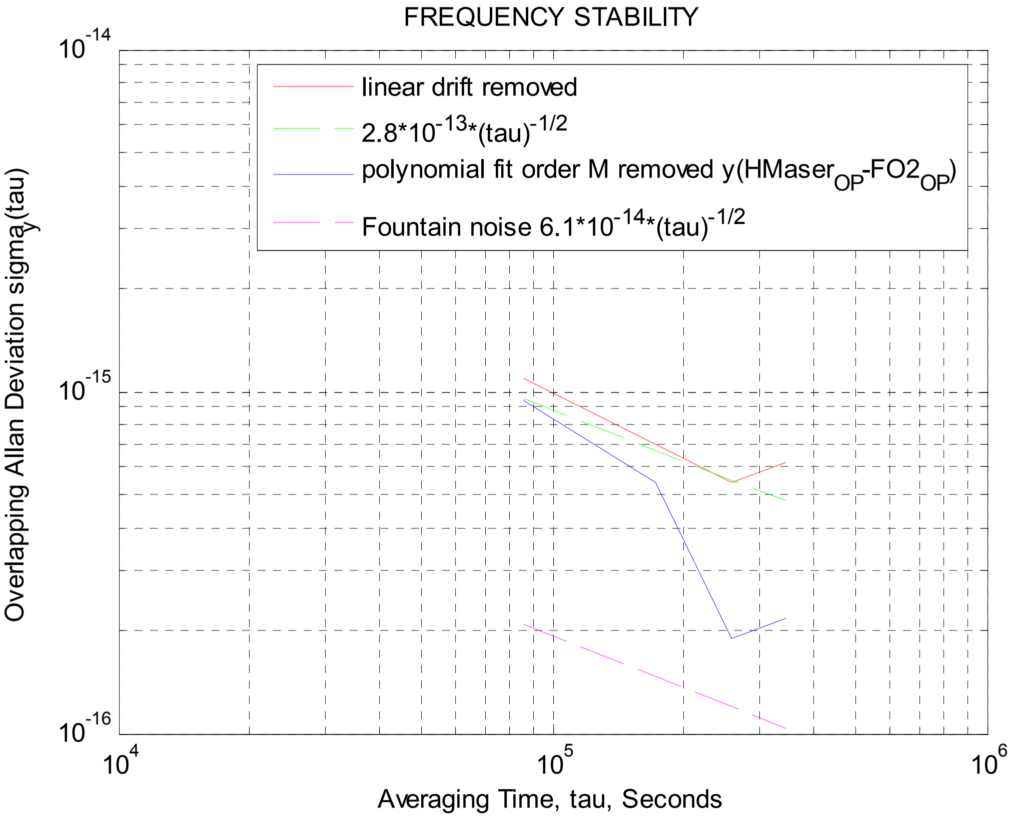

Figure 12: Comparison of frequency stability y(HMaser805 – FO2) polynomial order 2 and order M=11 removed from MJD 53379 to MJD 53399

Mean Frequency computed by phase differences

Figure 13 shows the evolution of the differences in fractional frequency y(t). At each period of integration is evaluated a frequency $\tilde{y}_k$ corresponding to the interval $t_{k+1} - t_k$. The relation binding the variations of phase and the instantaneous frequency deviations is given by

$$y_k = \frac{x_{k+1} - x_k}{t_{k+1} - t_k} \tag{1}$$

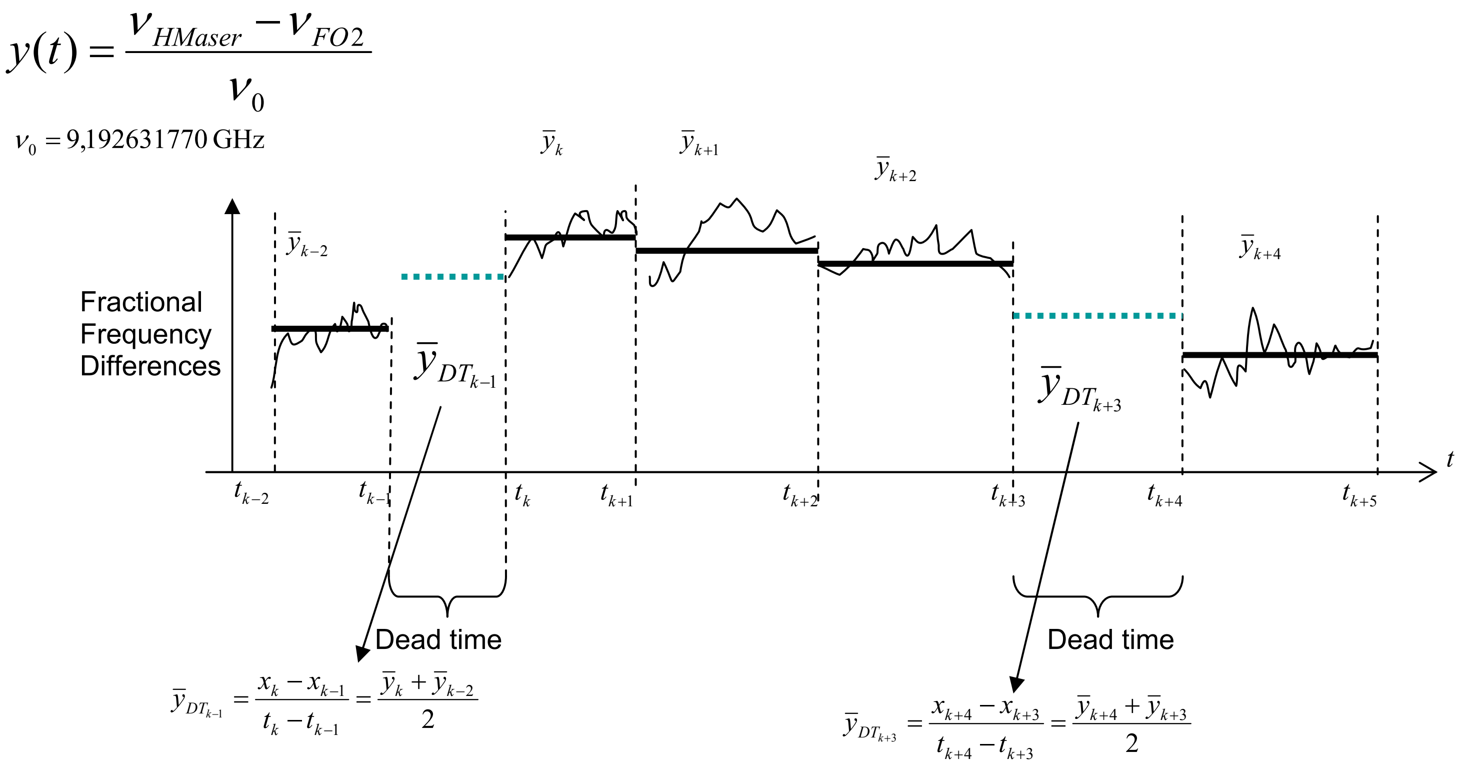

Figure 13: contribution of frequency measurements on the mean frequency calculated

By using equation (1) we have $x_{k+1} - x_k = (t_{k+1} - t_k)\, y_k$

and for addition of consecutive phase differences we find $\sum_{k=1}^{N} (x_{k+1} - x_k) = x_{N+1} - x_1 = \sum_{k=1}^{N} (t_{k+1} - t_k)\, y_k$

During the dead time we have evaluated the mean frequency by interpolating the mean frequency between two neighbouring intervals of integrations noted:

$$y_{DT_{m-1}} = \frac{1}{2} y_m + \frac{1}{2} y_{m-1} \tag{2}$$

The contributions of N duty intervals with the frequency measurements y_k and *M* idle intervals with the mean frequency extrapolating between two neighbouring intervals of integration y_{DT} give the summation

$$\left(\sum_{k=1}^{N} (t_{k+1} - t_k)\, y_k \right) + \left(\sum_{m=1}^{M} (t_{m+1} - t_m)\, y_{DT_m} \right) = x_{fin} - x_{deb} \tag{3}$$

$$\boxed{y_{moy} = \frac{x_{fin} - x_{deb}}{86400\ MJD_{fin} - 86400\ MJD_{deb}}} \tag{4}$$

Where ($x_{fin} - x_{deb)}$) represents the phase variation between the whole period of integration.

The evaluation of statistical uncertainty on each phase differences data extracted from fractional frequency differences, as we have in presence of white frequency noise (WFM) in each period of measurement, is given by the expression

$$\sigma_x(\tau_i)^2 = \sigma_y(\tau_i)^2 \tau_i^2$$

For the whole period T of measurement that gives in frequency instability

$$\sigma_y(\tau) = \frac{\sqrt{\sum_{i=1}^{N} \sigma_y(\tau_i)^2 \tau_i^2}}{T}$$

With N =21, from the 9th to 29th January and $T = 86400\ MJD_{fin} - 86400\ MJD_{deb} = 1804200$ seconds it gives

$$\sigma_y(\tau) = \frac{\sqrt{\sum_{i=1}^{21} \sigma_y(\tau_i)^2 \tau_i^2}}{T} = 0.419\ 10^{-16}$$

$$\boxed{\sigma_A = 0.419\ 10^{-16}}$$

The evaluation of the mean frequency between two intervals of integrations during the period from MJD 53379 to MJD 53399 is given by equation (2) and calculated for frequency fluctuation difference measurements. Figure 14 shows the frequency differences between H_Maser 1400805 and FO2 (blue plus) and the mean frequency during dead times (magenta stars).

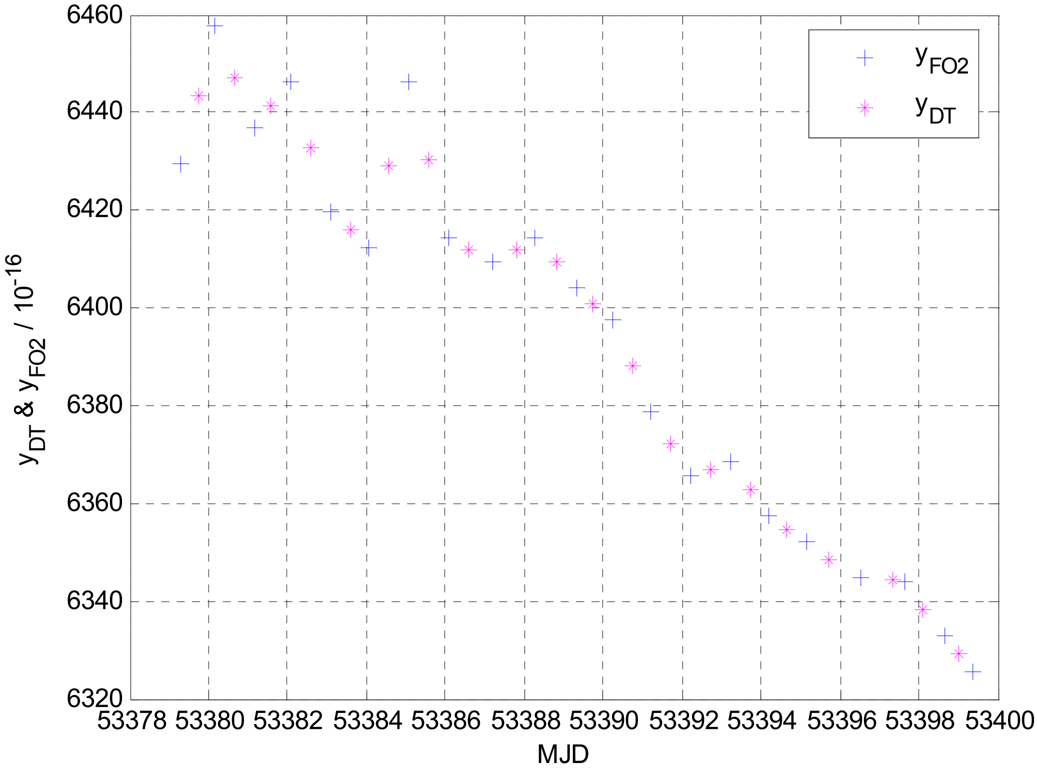

Figure 14: frequency differences H_Maser1400805 and FO2 from MJD 53379 up to MJD 53399

From equation (3) we find the phase difference over the whole period of integration

$$x_{fin} - x_{deb} = 1.153445\ \mu s$$

This value is replaced in equation (4) above for computation of y_{moy} during this period. We find

$$\boxed{y_{moy} = 0.639311\ 10^{-12}}$$

Mean Frequency between H Masers 1400805 and 1400816 computed by phase differences over MJD 53371 to 53401

On figure 15 is shown the evolution of the differences between phase differences $x_{[k]}$(H805)- $x_{[k]}$(H816) with a periodic measurement of 100s. From MJD_{deb} 53371,00048 up to MJD_{fin} 53401,99937 results N=26783 samples.

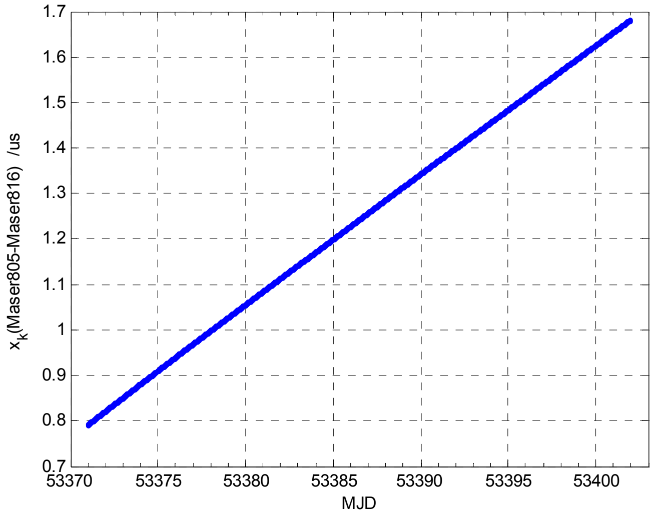

Figure 15: Phase differences Maser805-Maser816, MJD 53371 up to MJD 53401

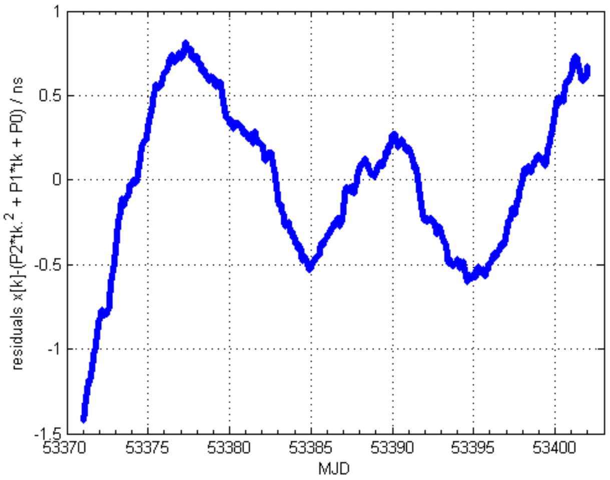

Figure 16: residuals of phase between Masers after quad fit removed, MJD 53371 up to MJD 53401

By using a second order polynomial fitting the phase differences data $x_{[k]}$(H805)- $x_{[k]}$(H816) : $x(t) := P_1\, t^2 + P_2\, t + P_3$

P1 = -2.32868827084747e-011; P2 = 2.5150563252857e-006; P3 = - 0.0678984405180812;

The mean frequency with this polynomial fit order 2 over the phase differences is given by:

$$y_{moy} = \frac{1}{86400}\left(\frac{1}{MJD_{fin} - MJD_{deb}} \int_{MJD_{deb}}^{MJD_{fin}} 2\, P_1\, t + P_2\, dt\right)$$ which is equivalent to

$$y_{moy} = \left(\frac{1}{86400} MJD_{deb} + \frac{1}{86400} MJD_{fin}\right) P_1 + \frac{1}{86400} P_2$$

Figure 16 shows residuals obtained after this quadratic fit removed. The 2 *ns* pick to pick residuals results to a frequency instability over the 53371 to 53401 period of 30 days of 7,71 x 10^{-16} .

➔ $(y_k)_{moy}$= 3315,51 x 10^{-16} ± 7,71 x 10^{-16}

By taking the restrictive period of 21 days 53379 to 53399 we find

➔ $(y_k)_{moy}$= 3297,22 x 10^{-16} ± 5,51 x 10^{-16}

Frequency difference between Masers obtained by first phase difference between beginning and ending of the whole period gives ➔ **$(y_k)_{moy}$= 3323,34 x 10^{-16}** with statistical uncertainty corresponding to $u_A(y_k)_{moy}=2\sigma_{meas}/T$ with σ_{meas} = 2ps of the time interval counter Stanford Research SR620 and T= 2678304s ➔ **$u(y_k)_{moy}$ = 1,5 x 10^{-18}**.

$$y_{H805-H816} = 0.332334\ 10^{-12} \qquad u_A(y_{H805-H816}) = 0.15\ 10^{-17}$$

By taking the restrictive period of 21 days 53379 to 53399 we find

$$\boxed{y_{H805-H816} = 0.329824\ 10^{-12}} \qquad \boxed{u_A(y_{H805-H816}) = 0.2205\ 10^{-17}}$$

Systematic error is evaluated with the time interval error of the time interval counter Stanford Research SR620:

Error < ± (500 ps typ. [1 ns max.] + Timebase Error ´ Interval + Trigger Error)

Considering the 3σ time interval error equal to 1 ns, the 1σ = 333,33ps. The evaluation of Time base Error is 1,35ps and the Trigger error is 0,23ps on input A and 0,23ps on input B of the counter. So we obtain $\sigma_{x(Counter)}(1\sigma)$ = 335 ps that is divided by a factor 100 corresponding to the phase difference multiplication used with the counter. From the frequency mean resulting from the first phase difference between the whole interval periods, the uncertainty is computed by

$$\sigma_B(yk)_{moy} = 2\sigma_{x(Counter)}/T \Rightarrow u_B(y_{H805-H816}) = 0.250\ 10^{-17}$$

By taking the restrictive period of 21 days 53379 to 53399 we find

$$\sigma_B(yk)_{moy} = 2\sigma_{x(Counter)}/T \Rightarrow \boxed{u_B(y_{H805-H816}) = 0.369\ 10^{-17}}$$

This result can be verified in consistency with the daily measurements of phase differences between Masers and the atomic local time scale UTC(OP). The differences between the phase differences x_k(H805-UTC(OP)) and x_k(H816-UTC(OP)) is plotted on figure 17 from MJD 53371 and MJD 53401.

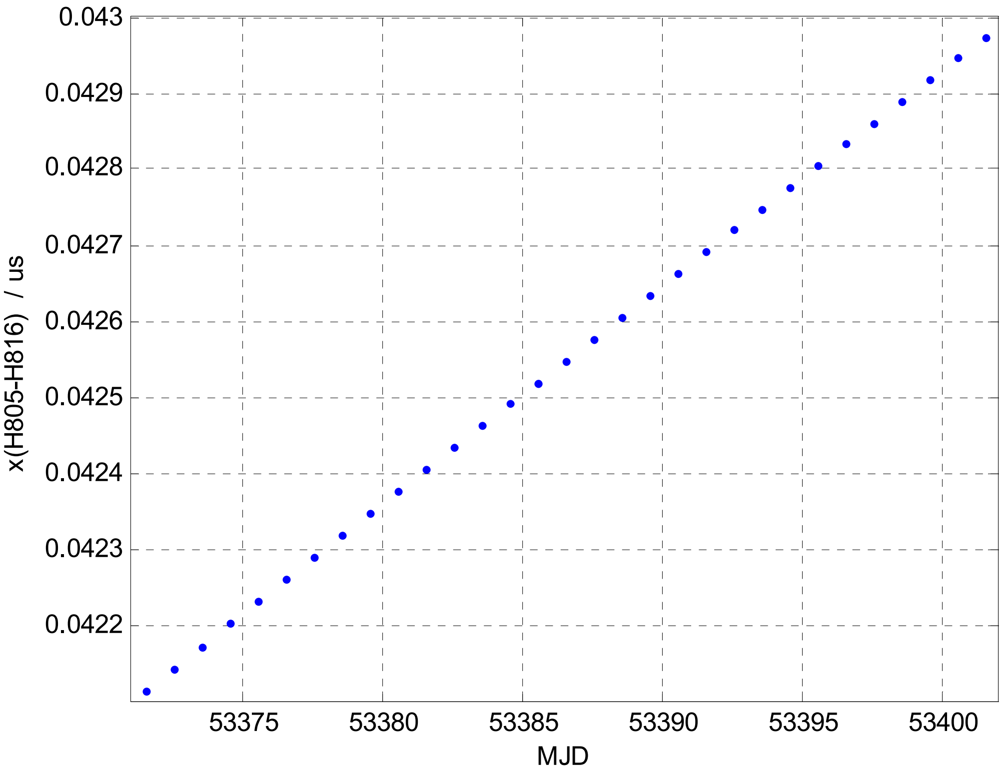

Figure 17: Phase differences (Maser805-UTC(OP)) – (Maser816 – UTC(OP)) , MJD 53371 up to MJD 53401

Frequency difference between Masers obtained by phase difference between beginning and ending of the 53371- 53401 period gives ➔ $(y_k)_{moy}$= **3321,76 x 10^{-16}** with statistical uncertainty corresponding to u_x =sqrt(2).u_x(t) with u_x(t)=150ps ➔ u_x=212ps and over the 30 days of the whole period $u_y(y_{moy})$ = 0,82 x 10^{-16} . The mean frequency obtains by these daily phase difference measurements Maser-UTC(OP) is resumed by:

➔ **$(y_k)_{moy}$= 3321,76 x 10^{-16} ± 0,82 x 10^{-16}**

The frequency difference between these two frequency averages is 1,58 x 10^{-16} that is compatible with their respective uncertainties.

By taking the restrictive period of 21 days 53379 to 53399 we find

➔ **$(y_k)_{moy}$= 3298,61 x 10^{-16} ± 1,17 x 10^{-16}**

The frequency difference between these two frequency averages is -0,37 x 10^{-16} that is compatible with their respective uncertainties.

REFERENCES

[ref. 1] - C. Vian, P. Rosenbusch, H. Marion, S. Bize, L. Cacciapuoti, S. Zhang, M. Abgrall, D. Chambon, I. Maksimovic, P. Laurent, G. Santarelli, A. Clairon of Obs. Paris, SYRTE, A. Luiten, M. Tobar, Univ. W. of Australia School of Physics, C. Salomon of LKB, "BNM-SYRTE Fountains: Recent Results", to be published in **Proceedings CPEM 2004**.

[ref. 2] - F. Pereira Do Santos, H. Marion, M. Abgrall, S. Zhang, Y. Sortais, S. Bize, I. Maksimovic, D. Calonico, J. Grünert, C. Mandache, C. Vian, P. Rosenbusch, P. Lemonde, G. Santarelli, Ph. Laurent and A. Clairon of BNM-SYRTE, C. Salomon of LKB, "Rb and Cs Laser Cooled Clocks: Testing the Stability of Fundamental Constants". **Proceedings IEEE 2003, EFTF Tampa May 2003, p 55-67.**

[ref. 3] - P. Wolf of BNM SYRTE, C.J. Bordé of LPL, "Recoil effects in microwave Ramsey spectroscopy", arxiv: **quant-ph/0403194**.

[ref. 4] - F. Pereira Do Santos, H. Marion, S. Bize, Y. Sortais, A. Clairon, and C. Solomon "Controlling the Cold Collision Shift in High Precision Atomic Interferometry" of, **Phys, Rev, Lett, 89,233004 (2002)**.

[ref. 5] - J. Vanier, C. Audouin, « The Quantum Physics of Atomic Frequency Standards », **Adam Hilger, Bristol & Philadelphia (1989)**.

[ref. 6] - R. Schröder, U. Hübner and D. Griebsch, "Design and Realization of the Microwava Cavity in PTB Caesium Atomic Clock CSF1" **IEEE Trans. Instrum. Meas., vol. 49, p.383, 2002**.

[ref. 7] - L. Cutler *et al*, "Frequency pulling by hyperfine σ - transitions in cesium atomic frequency standards, **J. Appl. Phys. Vol. 69, pp. 2780, 1991**.

[ref. 8] - A. Bauch, R. Schröder "Frequency shift in Caesium Atomic Clock due to Majorana transitions", Annalen der Physik**, vol. 2, pp. 421, 1993**.

[ref. 9] – H. Marion thèse de doctorat de l'Université de Paris 6 (To be published)